

Characterization of dehydrated sodium-containing catalysts by ^{23}Na solid-state NMR

Spectroscopic background: ^{23}Na nuclei have a spin of $I = 3/2$ and a quadrupole moment of $Q = 10.4 \times 10^{-30} \text{ m}^2$. Therefore, ^{23}Na NMR signals of sodium atoms in dehydrated solids are affected by quadrupolar interactions. The ^{23}Na isotope has a natural abundance of 100 % and a sensitivity of 9.3×10^{-2} in comparison with ^1H nuclei (1.0), making this isotope a very suitable candidate for NMR studies of solids. For basic principles of solid-state NMR, see lectures “Solid-State NMR Spectroscopy” for Bachelor students or PhD seminars, accessible via the link “Lectures for Students”.

If a catalyst framework contains atoms, which cause **negative framework charges**, **these charges are compensated by extra-framework cations**, such as Li^+ , Na^+ , Cs^+ , Ca^{2+} , Mg^{2+} etc. Extra-framework cations in zeolites are coordinated with framework oxygen atoms and located on well-defined cation sites of the zeolite structure (see **Fig. 1** for the faujasite structure of zeolites X and Y [1]). At ambient temperature, exchange of extra-framework cations between different crystallographically non-equivalent sites can be neglected on the time scale of NMR spectroscopy. In this case, the solid-state NMR spectra, e.g. of sodium cations, are mainly determined by the strength of their quadrupolar interactions, making this method a powerful tool for structure studies [1-10]. The **quadrupole coupling constants, C_Q , depend on the electric field gradients**, which in a first approximation are caused by a superposition of the electrostatic fields of the negatively charged framework oxygen atoms. Simply, the **C_Q value is large for sodium cations, which are unsymmetrically coordinated to oxygen atoms**, e.g.

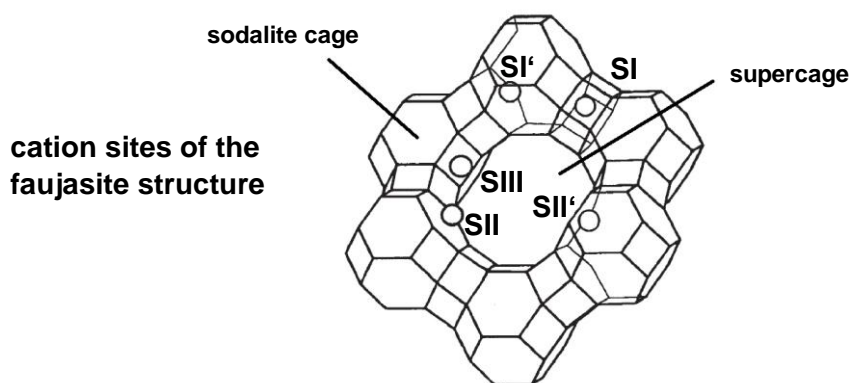


Fig. 1

outside of the center of a 6-membered oxygen ring (positions SII in zeolite Y, see **Fig. 1**) and **small for a symmetric oxygen surrounding**, e.g. for octahedrally coordinated sodium cations (positions SI in zeolite Y, see **Fig. 1**) [1]. In the first case, the electric field gradient at the cation sites SII is large, while it is small in the latter case. Therefore, the C_Q value is a characteristic spectroscopic parameter for cations located at different crystallographic cation sites in zeolites. For hydrated zeolites, however, the importance of this spectroscopic parameter is lost, because of an averaging of the local electric field gradients at the different cation sites by mobile water molecules.

An experimental proof of the dominating role of quadrupolar interactions for ^{23}Na MAS NMR spectroscopy of sodium cations in dehydrated zeolites is given by **Fig. 2**. This Figure shows ^{23}Na MAS NMR spectra of sodium cations in dehydrated zeolite Na-Y, recorded at Larmor frequencies of $\nu_0 = 79.3$ to 198.4 MHz, i.e. utilizing magnetic fields of $B_0 = 7.0$ to 17.6 T (Fig. 1 of Ref. [11]). These spectra demonstrate that the **center of gravity of the ^{23}Na solid-state NMR signals is high-field shifted and the quadrupole patterns become narrow for increasing B_0 values**, which is typically caused by the second-order quadrupolar effect.

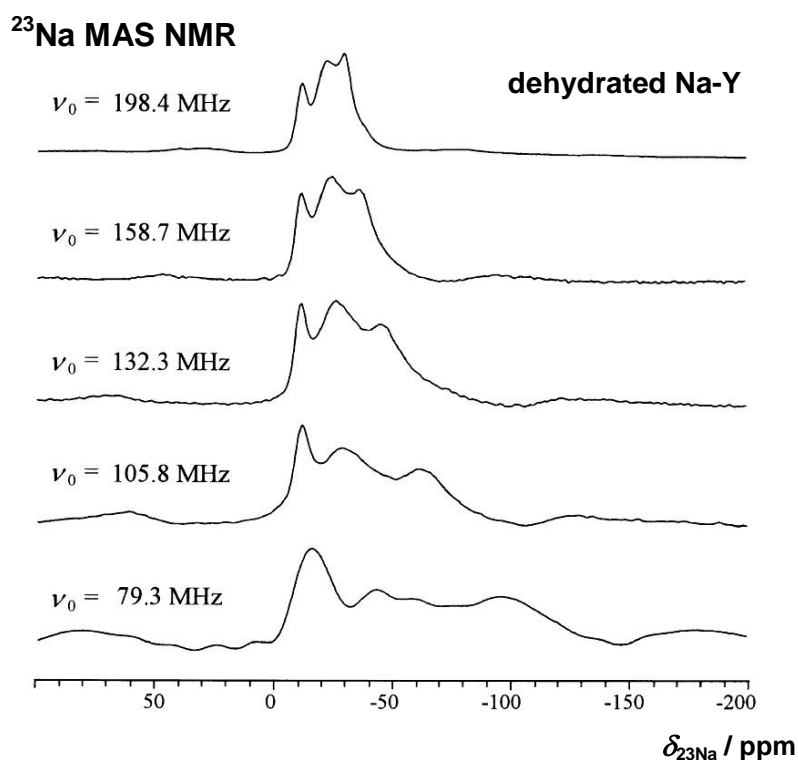


Fig. 2

The number and parameters of ^{23}Na MAS NMR signals contributing to spectra like those in **Fig. 2**, is often investigated by two-dimensional (2D) MQMAS NMR experiments. In **Fig. 3**, the 2D ^{23}Na ORIACT MQMAS NMR spectrum of a dehydrated zeolite Na-Y with $n_{\text{Si}}/n_{\text{Al}} = 2.5$ is shown [8]. This spectrum consists of three peaks. For details of ORIACT (Off-resonance Rotation-Induced Adiabatic Coherence Transfer) MQMAS experiments, see Ref. [12].

2D ^{23}Na ORIACT MAS NMR

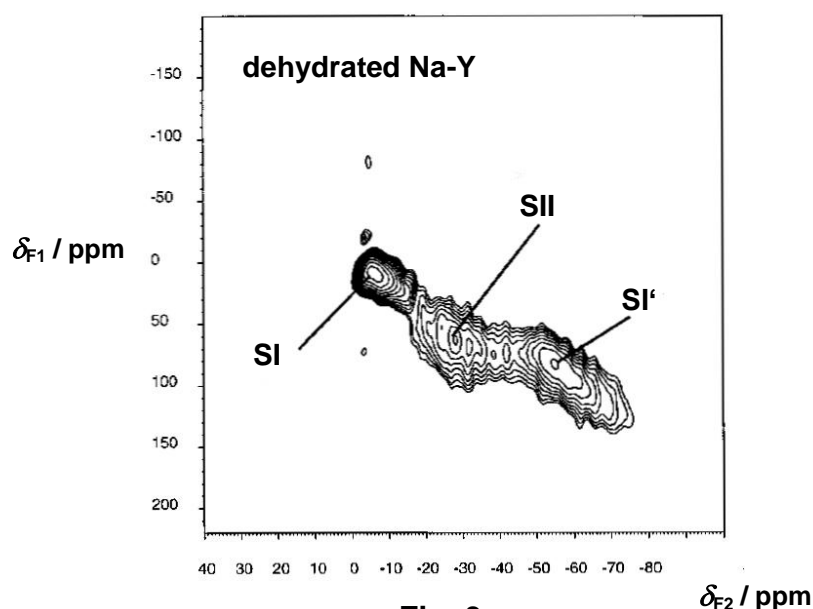
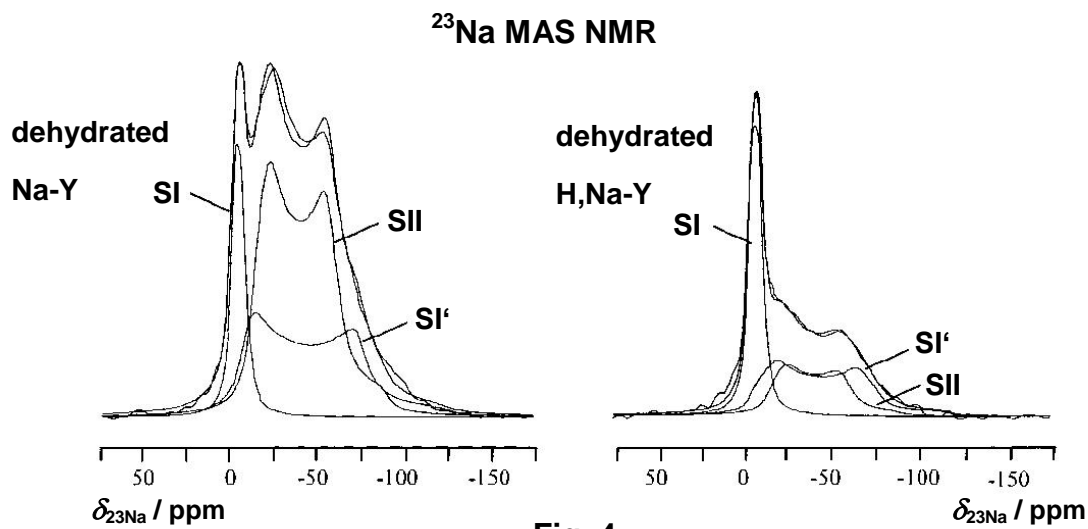


Fig. 3

Quantitative evaluation of the 2D ^{23}Na ORIACT MQMAS NMR spectrum in **Fig. 3** delivered the isotropic chemical shifts $\delta_{23\text{Na,iso}}$, and the *SOQE* parameters (Second-Order Quadrupolar Effect) of the signals responsible for the three peaks. These data are helpful for the simulation of one-dimensional ^{23}Na MAS NMR spectra. **Fig. 4** demonstrates the results of this procedure for the signal separation in the ^{23}Na MAS NMR spectra of dehydrated faujasite-type zeolites Na-Y and H,Na-Y (both $n_{\text{Si}}/n_{\text{Al}} = 2.5$). The signal separation shown in **Fig. 3** is a prerequisite for determining the relative signal intensities and, utilizing the total sodium concentration determined by chemical analysis, the population of sodium cations at the different crystallographically non-equivalent cation sites.

Due to the large number of cation sites in zeolites, such as shown in **Fig. 1** for the faujasite structure, it is a complex topic to attribute the various ^{23}Na MAS NMR signals to cations at the specific crystallographic sites. A helpful procedure can be

^{23}Na MAS NMR studies of cation-exchanged zeolites. In the spectrum of dehydrated zeolite H,Na-Y in **Fig. 4, right**, the intensities of the quadrupolar patterns at the right-hand side are much weaker in comparison with those in the spectrum of zeolite Na-Y in **Fig. 4, left** [8]. This finding indicates that the quadrupolar patterns must be due to sodium cations at SII and/or SI' sites, because sodium cations at these sites are preferentially exchanged by hydroxyl protons in faujasite zeolites [8].



Furthermore, applying the point charge model described in Ref. [13] as well as using the atomic coordinates given for the faujasite structure in Ref. [14], and oxygen net charges of -0.8 e , the local electric field gradients at the cation sites of zeolite structures and the quadrupole couplings constants of sodium cations, located at these sites, were calculated. In **Table 1**, column 2, the results of such point charge

Zeolites / Sites	Calculated C_Q / MHz	Experimental C_Q / MHz	Experimental η_Q	Experimental $\delta_{23\text{Na},\text{iso}}$ / ppm	Refs.
NaY (2.5)*					
SI	0.1 – 0.5	0.1	0	-12	[4]
SI'	4.6 – 5.6	4.8	0.2	-4	[4]
SII	3.4 – 4.2	4.2	0.2	-12	[4]
NaX (1.2)*					
SI	0.2	0.1	0	-6	[4]
SI'	3.6 – 5.2	5.2	0	-19	[4]
SII	4.4	4.6	0	-16	[4]
SIII	2.2 – 2.5	ca. 2.4	0.8	-30 to -16	[4]

Na-LSX (1.0)*					
SI		1.2	0.1	0	[8]
SI'		5.9	0.1	-6	[8]
SII		5.1	0.2	-12	[8]
SIII'(1,2)		2.2	0.5	-13	[8]
SIII'(3)		2.0	0.8	-1	[8]
H,Na-Y (75)**					
SI		1.2	0.1	-3	[8]
SI'		4.9	0.3	5	[8]
Na-MOR (7)*					
SI		2.9	0.6	-24	[10]
SIV		2.9	0.5	-19	[10]
SVI		2.3	0.6	-12	[10]
Na-ZSM-5 (18)* in 10-rings		2.0***		-18.0	[5]
Na-FER (27)*					
SI		4.3	0.6	-1.5	[15]
SIIa		2.2	0.6	-15.5	[15]
SIIb		2.1	0.6	-19.5	[15]
SIII		3.6	0.6	-22.5	[15]
Na-Saponite signal 1 signal 2		1.2 2.5	1.0 0.5	-7 -3	[16] [16]
Na-Stevensite signal 1 signal 2		2.7 2.7	0.5 0.8	-2 -20	[16] [16]
Na-Hectorite signal 1 signal 2 signal 3		1.8 1.6 1.7	0.3 0.2 0.3	0 -14 -25	[16] [16] [16]

*) $n_{\text{Si}}/n_{\text{Al}}$ ratio

**) cation exchange degree

***) SOQE values determined via 2D ^{23}Na MQMAS NMR spectroscopy

Table 1

calculations for sodium cations in zeolites Na-Y and Na-X are summarized [4]. The comparison of calculated (second column) and experimentally (third column) derived quadrupole coupling constants allows the assignment of ^{23}Na MAS NMR signals to the various cation sites (first column).

Utilizing the above-mentioned combination of experimental and theoretical approaches, the investigation of cation populations of sodium-containing zeolites with a larger number of crystallographically non-equivalent cation sites is possible. **Fig. 5** shows the ^{23}Na MAS NMR spectra of a dehydrated zeolite **Na-X** with $n_{\text{Si}}/n_{\text{Al}} = 1.2$, recorded at Larmor frequencies of $\nu_0 = 105.8$ MHz (bottom) and 158.7 MHz (top) (Fig. 2 of Ref. [4]). The high-field range of the spectra consists of two patterns corresponding to **C_Q values of ca. 4.6 MHz and 5.2 MHz**, which are caused by sodium cations located on **SII and SI' sites**, respectively. In the low-field range, very weak signals appear due to sodium cations located at SI sites. In contrast to the ^{23}Na MAS NMR spectra of dehydrated zeolite Na-Y, at least two additional structureless signals of sodium cations located on **SIII sites** were found, corresponding to **C_Q values of ca. 2.4 MHz**.

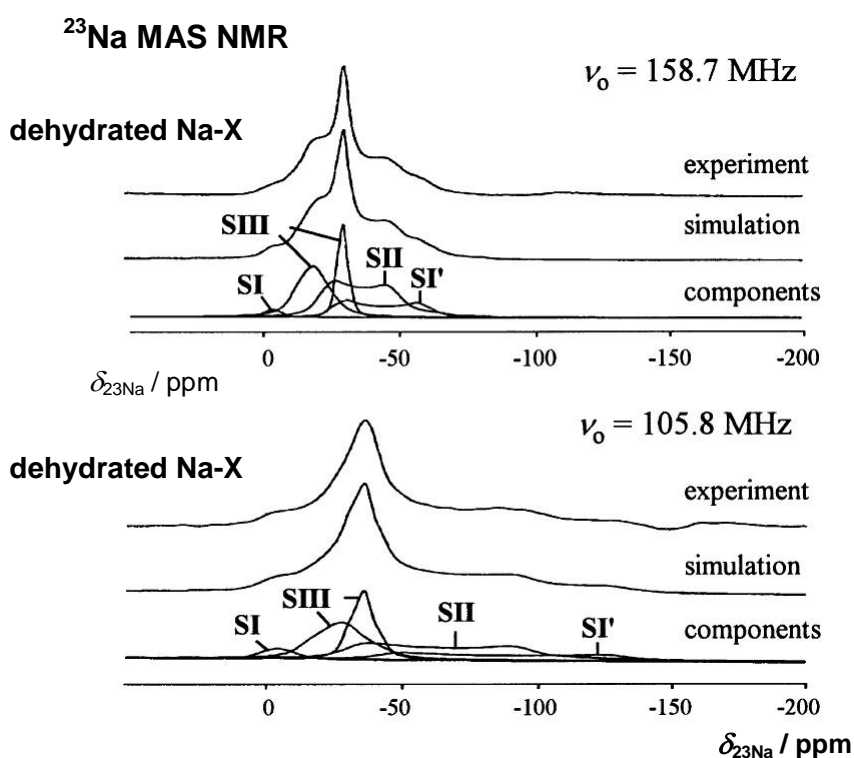


Fig. 5

In **Table 1, bottom lines**, ^{23}Na solid-state NMR parameters of further zeolites and porous materials, investigated in the dehydrate state, are given. For ^{23}Na solid-state NMR studies of sodium cations in hydrated zeolites, see Refs. [2], [3], and [17]. For a general survey on ^{23}Na solid-state NMR parameters of sodium atoms in solids, see Table 8.2 in Ref. [18].

Catalyst preparation: The observation of the quadrupole patterns of sodium cations at crystallographically non-equivalent sites requires a dehydration of the powder samples, e.g. via a standard dehydration inside a “sample tube system 1” at the “vacuum line 1” (see Sections “sample tube system 1” and “vacuum line 1”, accessible via the link “*In Situ* Solid-State NMR Techniques”). The dehydration starts with an evacuation at room temperature for ca. 10 minutes followed by a temperature ramp from room temperature to $T = 393$ K within 2 hours. At this temperature, the sample was dehydrated for 2 hours. Subsequently, the temperature was increased up to $T = 723$ K within 3 hours and evacuated at this temperature for 12 hours. After this treatment, the sample tube system was closed via the vacuum valve and disconnected from the vacuum line (after this line was ventilated with air). The transfer of the dehydrated sample into the MAS NMR rotor was performed without air contact in a mini glove box (see Section “mini glove box”, accessible via the link “*In Situ* Solid-State NMR Techniques”), purged with dry nitrogen gas.

^{23}Na solid-state NMR studies: Due to the quadrupolar interactions of ^{23}Na nuclei, their single pulse excitation was performed by less than $\pi/4$ and most suitable by $\pi/8$ pulses. Often, a repetition time of $t = 1$ to 2 s was used. For reaching a suitable resolution of the ^{23}Na MAS NMR spectra, the sample spinning rate has to be as high as possible and at least $\nu_{\text{rot}} = 10$ kHz. The 2D ^{23}Na ORIACT MQMAS experiments were performed with a two-pulse p_1 - t_1 - p_2 -sequence and an appropriate phase cycling [8]. The pulse durations p_1 and p_2 were set to 3 to 5 μs and 25 μs with radio frequency power levels corresponding to $\nu_{\text{rf}} = 150$ and 75 kHz, respectively. The value of p_1 was optimized to maximize the relative contribution of the broad signals. The value of p_2 is bound by the RIACT condition, i.e. equal to a quarter of the rotor period. A spectral width of 750 ppm, corresponding to an increment of 6.3 μs for t_1 , was used for the F1 dimension, with a total of 32 increments. The carrier frequency was chosen to be about 4 kHz off-resonance, which is a value suitable for large quadrupolar coupling constants. For each t_1 increment, a number of scans between 20 (typical) and 900 (for very low sodium contents) were used. The repetition time was set to 500 ms [8]. Referencing of the chemical shift was performed to 1 M aqueous solution of NaCl ($\delta_{^{23}\text{Na}} = 0$ ppm) or solid NaCl, which has a ^{23}Na chemical shift of $\delta_{^{23}\text{Na}} = 7.21$ ppm.

References:

- [1] M. Hunger, G. Engelhardt, H. Koller, J. Weitkamp, *Characterization of sodium cations in dehydrated faujasites and zeolite EMT by ^{23}Na DOR, 2D nutation, and MAS NMR*, Solid State Nucl. Magn. Reson. 2 (1993) 111-120, DOI: 10.1016/0926-2040(93)90029-M.
- [2] M. Hunger, G. Engelhardt, J. Weitkamp, *Cation migration in zeolite LaNaY investigated by multi-nuclear solid-state NMR*, Stud. Surf. Sci. Catal. 84A (1994) 725-732, DOI: 10.1016/S0167-2991(08)64179-8.
- [3] H. Klein, H. Fuess, M. Hunger, *Cation location and migration in lanthanum-exchanged zeolite NaY investigated by X-ray powder diffraction and MAS NMR spectroscopy*, J. Chem. Soc., Faraday Trans. 91 (1995) 1813-1824, DOI: 10.1039/ft9959101813.
- [4] M. Feuerstein, M. Hunger, G. Engelhardt, J.P. Amoureux, *Characterization of sodium cations in dehydrated zeolite NaX by ^{23}Na NMR spectroscopy*, Solid State Nucl. Magn. Reson. 7 (1996) 95-103, DOI: 10.1016/S0926-2040(96)01246-5.
- [5] M. Hunger, P. Sarv, A. Samoson, *Two-dimensional triple-quantum ^{23}Na MAS NMR spectroscopy of sodium cations in dehydrated zeolites*, Solid State Nucl. Magn. Reson. 9 (1997) 115-120, DOI: 10.1016/S0926-2040(97)00051-9.
- [6] K.-N. Hu, L.-P. Hwang, *The influence of adsorbed molecules on Na-sites in NaY zeolite investigated by triple-quantum ^{23}Na MAS NMR spectroscopy*, Solid State Nucl. Magn. Reson. 12 (1998) 211–220, DOI: 10.1016/S0926-2040(98)00065-4.
- [7] K.H. Lim, C.P. Grey, *Characterization of extra-framework cation positions in zeolites NaX and NaY with very fast ^{23}Na MAS and multiple quantum MAS NMR spectroscopy*, J. Am. Chem. Soc. 122 (2000) 9768-9780, DOI: 10.1021/ja001281d.
- [8] S. Caldarelli, A. Buchholz, M. Hunger, *Investigation of sodium cations in dehydrated zeolites LSX, X, and Y by ^{23}Na off-resonance RIACT triple-quantum and high speed MAS NMR spectroscopy*, J. Am. Chem. Soc. 123 (2001) 7118-7123, DOI: 10.1021/ja0102538.
- [9] L. Gueudre, A.A. Quoineaud, G. Pirngruber, P. Leflaive, *Evidence of multiple cation site occupation in zeolite NaY with high Si/Al ratio*, J. Phys. Chem. C 112 (2008) 10899–10908; DOI: 10.1021/jp803037u.
- [10] B. Fan, W. Zhang, P. Gao, G. Hou, R. Liu, S. Xu, Y. Wei, Z. Liu, *Quantitatively mapping the distribution of intrinsic acid sites in mordenite zeolite by high-field ^{23}Na solid-state nuclear magnetic resonance*, J. Phys. Chem. Lett. 13 (2022) 5186–5194, DOI: 10.1021/acs.jpclett.2c00932.

- [11] G. Engelhardt, M. Hunger, H. Koller, J. Weitkamp, *Exploring cation siting in zeolites by solid-state NMR of quadrupolar nuclei*, Stud. Surf. Sci. Catal. 84A (1994) 421-428, DOI: 10.1016/S0167-2991(08)64141-5.
- [12] S. Caldarelli, F. Ziarelli, *Spectral editing of solid-state MAS NMR spectra of half-integer quadrupolar nuclei*, J. Am. Chem. Soc. 122 (2000) 12015-12016, DOI: 10.1021/ja0029127.
- [13] H. Koller, G. Engelhardt, A.P.M. Kentgens, J. Sauer, ^{23}Na NMR spectroscopy of solids: Interpretation of quadrupole interaction parameters and chemical shifts, J. Phys. Chem. 98 (1994) 1544-1551; DOI: 10.1021/j100057a004.
- [14] D. Olson, *The crystal structure of dehydrated NaX*, Zeolites 15 (1995) 439-443, DOI: 10.1016/0144-2449(95)00029-6.
- [15] P. Klein, J. Dedecek, H.M. Thomas, S.R. Whittleton, J. Klimes, J. Brus, L. Kobera, D.L. Bryce, S. Sklenak, *NMR crystallography of monovalent cations in inorganic matrices: Na^+ siting and the local structure of Na^+ sites in ferrierites*, J. Phys. Chem. C 126 (2022) 10686-10702, DOI: 10.1021/acs.jpcc.2c02496.
- [16] K. Sato, K. Numata, W. Dai, M. Hunger, *Tunable states of interlayer cations in two-dimensional materials*, Appl. Phys. Lett. 104 (2014) 131901, DOI: 10.1063/1.4870006.
- [17] A. Seidel, U. Tracht, B. Boddenberg, *Study of the dispersion of sodium chloride in zeolite NaY*, J. Phys. Chem. 100 (1996) 15917-15922, DOI: 10.1021/jp9610731.
- [18] D. Freude, <https://www.dieter-freude.de/quad-nmr>.